

Influence of Infill Parameters on the Tensile Mechanical Properties of 3D Printed Parts

Rachel Guan ¹, Damon Smith ²

¹Haynes Academy, Metairie, LA

²Department of Mechanical Engineering, University of New Orleans, New Orleans, LA

Correspondence:

Damon Smith, Department of Mechanical Engineering, University of New Orleans, New Orleans, LA

Email: dsmith3@uno.edu

SUMMARY

Manufacturers that produce products using fused filament fabrication (FFF) 3D printing technologies have control of numerous build parameters. This includes the number of solid layers on the exterior of the product, the percentage of material filling the interior volume, and the many different types of infill patterns used to fill their interior. It is important that manufacturers understand how these choices affect the mechanical properties of the product, the amount of material needed, and how long it will take to print the part. This study tested the hypothesis that as the density of the part increases, the mechanical properties will improve at the expense of build time and the amount of material required. The mechanical strength and stiffness of printed test specimens in this study increased with increasing density. In addition, we found that adding more solid external layers to the specimens increased the strength-to-weight ratio. The ductility was much greater in the specimens with a rectilinear infill pattern possibly due to better pattern alignment of the object and better adhesion to the outer solid layers. This study supported our hypothesis and provides a guide for designers and engineers seeking to optimize tensile mechanical behavior, print time, and material usage for FFF applications through the selection of optimal infill parameters.

INTRODUCTION

Additive manufacturing (AM), known more commonly as 3D printing, is a transformative technology that offers many distinct advantages over traditional manufacturing techniques such as machining or casting. Key advantages include reduced waste, reduced assembly, and the capability to produce complex geometries not feasible using other processes (1). AM works by translating a 3D computer model of an object into a physical object using a layer-by-layer fabrication method. Among the many AM systems currently available for consumers, fused filament fabrication (FFF) is the most popular due to the relative simplicity of the technique and the low cost of equipment and materials (1). FFF systems construct parts from a filament of a thermoplastic material heated and extruded in a layer-by-layer manner onto a build platform. Slicer software divides a 3D digital model of an object into

individual 2D layers of a specific thickness and generates the necessary machine instructions to print the part. In a typical FFF print, the top and bottom layers of an object are solid and the layers between these have a solid outer perimeter and a partially filled interior region (1). While it is possible to create a completely solid object, this is time prohibitive for many applications. To produce the final part more efficiently, the designer or engineer chooses the desired number of solid layers, infill percentage, and infill pattern. Most commercially available slicer packages contain a variety of infill patterns to choose from. Additional printer settings include nozzle temperature, build platform (or build chamber) temperature, and feed mechanism parameters such as print, feed, and retraction rates. These parameters can dramatically influence the print time, object density, and mechanical behavior of the part produced. For applications where an object has an applied external load, an understanding of how these parameters affect the mechanical behavior is particularly important.

There have been several studies that examine how FFF print parameters affect the outcome of printed objects (2-5). Much of the research focuses on the dependence of material fusion on the thermal properties and feed rate. For example, Costa et al. and Khaliq et al. studied how the FFF print parameters influenced the melt viscosity of the print materials and how this impacted the object microstructure (4, 5). By adjusting the melt viscosity for optimized interlayer fusion and fusion between adjacent deposits, or "roads", of the thermoplastic material, they found that the mechanical performance improved. Additional studies focus on the infill parameters that are available for designers and engineers (6-9). Fewer studies have assessed the effect of infill parameters on the mechanical behavior of FFF printed parts (10-12). To our knowledge, no studies exist that have simultaneously compared the ultimate tensile strength, elastic modulus, and ductility of different infill patterns, while also considering the time and material required to print each type of specimen. The ultimate tensile strength is the maximum stress, the force divided by cross-sectional area, recorded of a stretched test specimen before fracture and is important for applications where the printed part has an applied external load. The modulus is the ratio of stress and strain, the amount of elongation, of the specimen before it becomes permanently plastically deformed and is indicative of the stiffness of

a printed part. The strain at break is the amount of strain recorded when fracture of the specimen occurred and is an indication of the ductility of a part, or how much it will stretch before failure. Ductility is an important parameter for parts in load-bearing applications. Parts with ductility values that are too low can fail instantaneously without any prior indication of a problem. Herein, we test the hypothesis that the mechanical properties of the printed parts will improve as the density increases but will require more print time and material.

RESULTS

We measured the influence of 3D printer infill parameters on the mechanical properties of printed specimens by subjected them to a tensile force until fracture occurred. The infill percentage, corresponding to the amount of interior volume of the specimen filled, was varied for rectilinear, triangular, and honeycomb infill patterns (Figure 1). The number of outer exterior solid layers was also varied for the rectilinear infill pattern. The ultimate strength and the elastic modulus increased with increasing infill percentage for each of the different infill patterns examined (Figure 2A). The honeycomb pattern showed the greatest overall ultimate strength and elastic modulus compared to the other infill patterns. The triangular pattern showed greater ultimate strength and elastic modulus compared to the rectilinear pattern, except for the ultimate strength at the highest infill of 55%. For the rectilinear infill, we also observed a trend of increasing ultimate strength and modulus with an increase in the number of solid outer layers and the infill percentage held constant at 25%.

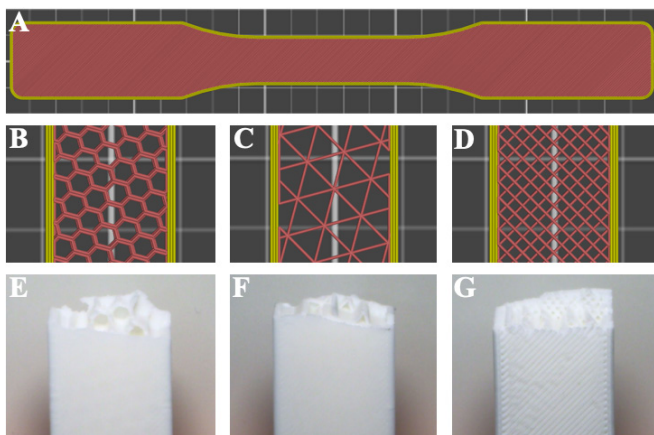


Figure 1: 3D Printed Test Specimens. Slicer software view of the (A) tensile test specimen with (B) honeycomb, (C) triangular, and (D) rectilinear infill patterns. Representative images of fractured test specimens with (E) honeycomb, (F) triangular, and (G) rectilinear infill patterns.

In the context of FFF printing, print speed often refers to the speed at which the print head travels linearly along the build platform. In this study print speed refers to the printed object volume per unit time, based on the outer geometry of the object. This data would be a useful metric

for manufacturers seeking to optimization production time. While the honeycomb pattern provided a greater strength and elastic modulus compared to the other infill patterns, it required a much longer print time to produce the object volume (Figure 2B). When comparing the results of the different rectilinear infill percentages to the 25% rectilinear specimens with varied numbers of solid outer shells, the ultimate strength increased with lower densities when using more solid outer layers. This resulted in a greater strength-to-weight ratio than achieved by increasing the infill percentage alone. While the ultimate strength and elastic modulus did vary based on the selection of the specific infill parameters chosen, these mechanical properties largely trended with the object density, as hypothesized (Figure 3).

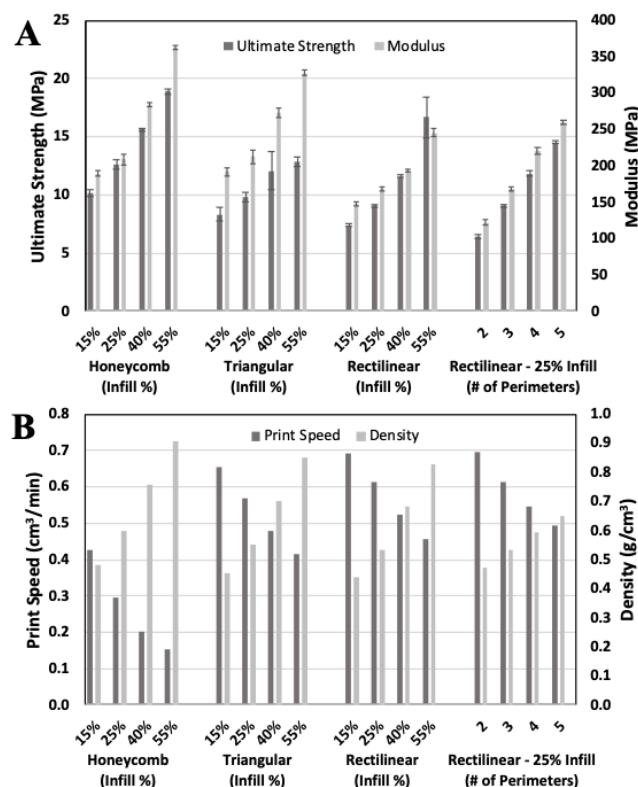


Figure 2: Overall Performance of Test Specimens. (A) Ultimate tensile strength and modulus of test specimens versus infill percentage and the number of solid outer layers. Error bars indicate the standard deviation (n= 5). (B) Print speed and object density versus infill percentage and the number of solid outer layers.

We compared the ductility of the specimens using the measured strain at break. Though a greater sample variability occurred for specimens printed with the rectilinear infill pattern, these specimens had an average strain at break that was higher than the other patterns, particularly for the 40% and 55% infills (Figure 4A). Notably, there was no observed dependence of ductility on the infill percentage for the honeycomb and triangular infills. Unlike the ultimate strength and modulus, there was no observable relationship between

the ductility of the specimens and their density (Figure 4B).

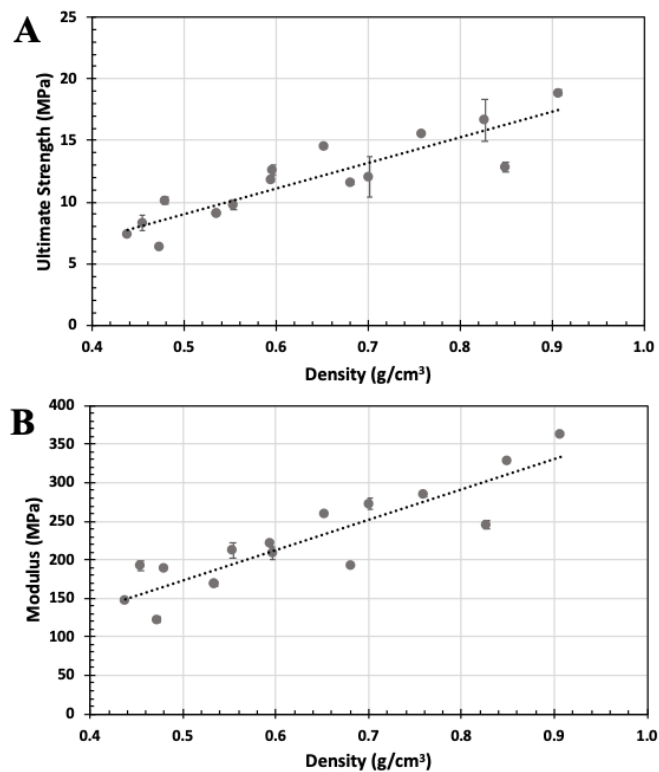


Figure 3: Mechanical Strength and Modulus Versus Test Specimen Density. (A) Ultimate tensile strength and (B) modulus of all infill patterns tested versus the specimen density. Error bars indicate the standard deviation (n=5) and dotted lines show linear fits with an R2 of 0.8. An increase in strength and modulus is observed with increasing density.

DISCUSSION

This study demonstrated the effect of several commonly modified print parameters on the tensile mechanical properties, build time, and amount of material needed for test specimens printed using an FFF printing system. There was a general trend observed that ultimate strength and elastic modulus increased with increasing infill percentage. For the same infill percentage, honeycomb patterns provided slightly higher ultimate strength and elastic modulus, followed by triangular and then rectilinear. However, we observed that this benefit in mechanical behavior came at a cost of increased print time. This resulted from the more frequent changes in direction of the printer head as it printed the more complex honeycomb geometry. In contrast, the print head moved in straight lines across the entire object layer before a directional change occurred when printing the triangular and rectilinear geometries. These patterns, therefore, showed much faster print speeds, with rectilinear being slightly faster than triangular. When the infill of a test specimen was constant and the number of outer solid shells varied, we observed a similar trend of increasing ultimate strength and elastic modulus. The data also showed a slightly higher strength-to-weight ratio

occurred by increasing the number of solid outer shells. While some overall variation existed between the different infills, the ultimate strength and elastic modulus largely trended with the specimen density. This indicated that the density of a printed object may be a more practical means of evaluating the relative mechanical behavior of an FFF printed part than the vast array of other possible infill parameters.

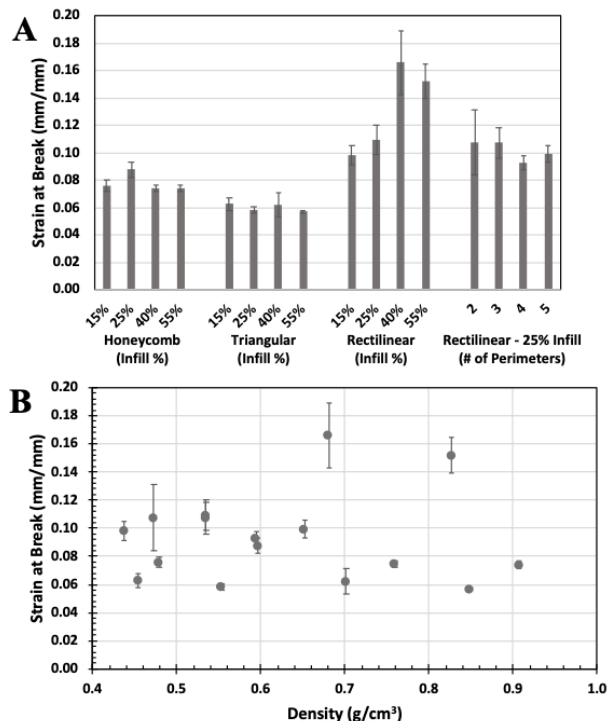


Figure 4: Ductility of Test Specimens. (A) Strain at break of the test specimens. (B) Strain at break of all infill patterns tested versus the specimen density. Error bars indicate the standard deviation (n=5). There was no observed dependence of ductility on specimen density.

The ductility of the specimens with rectilinear infill, evaluated by the strain at break, showed a much higher value than the honeycomb and triangular patterns. This was most apparent for the specimens with higher infill values but did not trend with increasing density as observed for ultimate strength and elastic modulus. One possible explanation for this result is the orientation of the infill angle with respect to the axis of strain. Due to the printing orientation, the rectilinear pattern has a more preferential alignment with the external applied load (Figure 1D-F). Each of the deposited roads of material are at 45 degrees to the tensile load axis, which would result in comparatively smaller bend angles for a given strain. This is consistent with the study by Górski et al. where a transition from brittle to ductile behavior occurred that was dependent on build orientation (13). It is also possible that the use of an infill pattern that is the same for the interior region and the solid surface layers results in better fusion between the surface layers and the infill. The lack of dependence of the ductility of the honeycomb and triangular patterns on the infill percentage would seem to indicate a stress concentration in

the geometry that leads to fracture which does not change when filled with more material. However, verification of the underlying mechanisms for the observed ductility requires further study.

This study provided a means of predicting the influence of infill settings on the mechanical behavior of polylactic acid (PLA) objects manufactured by FFF and may serve as a guide for designers and engineers to simplify the selection of print parameters. As an example, consider the design of printed coupling used to hang a light fixture and that requires a tensile stress of 10 MPa. The 25% honeycomb, 40% triangular, and 40% rectilinear infills with three perimeters meet the stress requirement (**Figure 2A**). The honeycomb option uses the least material with the lowest density, but the rectilinear is the faster printing option (**Figure 2B**). However, with an additional perimeter added to the rectilinear pattern, an infill of 25% meets the strength requirement. This provides a similar density to the honeycomb option and improves the print speed. These results provide a guide for additional design decisions based on the relative importance of weight, cost, speed, strength, stiffness, or ductility.

Overall, we found that the strength and modulus of printed objects increased with increasing specimen density, confirming our initial hypothesis. The print time and the amount of material required also increased with increasing density. The print time and strength-to-weight ratio of the specimens improved by increasing the number of solid outer layers. The ductility of the specimens, however, did not trend with density but were dependent on specific choices of infill percentage and pattern. The results of this study add to our current understanding of how 3D printer settings influence the underlying mechanisms that are responsible for the observed mechanical properties of printed objects. This knowledge is crucial as this manufacturing method continues to increase in popularity.

MATERIALS AND METHODS

Materials

The polylactic acid (PLA) filament used in this study was 1.75mm nominal diameter, purchased from 3D Solutech (Seattle, WA, USA).

Fused Filament Fabrication of Test Specimens

Test specimens were printed using a Prusa i3 MK3 FFF system equipped with a smooth polyetherimide (PEI) build platform and the printer setting indicated in Table 1. Specimens had outer geometries adhering to American Society for Testing and Materials (ASTM) D638-14 standard Type III (**Figure 1A**). Print parameters were set using Slic3r PE slicer software. The specimens were printed with the long axis of the samples aligned along the x-axis of the printer. The infill parameters varied in this study include infill pattern, infill percentage, and the number of exterior solid layers, which corresponds both to the number of perimeter shells and the number of top and bottom layers. Figure 1B, C, and

D show slicer software screen captures of the honeycomb, triangular, and rectilinear infills used in this study. These infills were selected based on their common inclusion in most slicer software. In all cases, the top and bottom layers were printed using the rectilinear pattern. It is common for pattern options to be different, and somewhat limited, for solid layers compared to the options for infill patterns. Rectilinear was chosen for the solid layers as it is the common default setting in many slicer software packages.

Material Characterization

FFF-printed tensile test specimens were tested based on the ASTM D638-14 standard test methods for tensile properties of plastics. The specimens were printed using the Type III specifications stated in the standard. Five specimens were tested for each of the infill conditions described. The printed specimens were removed from the printer and kept in dehumidifier cabinet at room temperature and 25% relative humidity for 24 hours prior to testing. Tensile testing of the specimens was conducted at room temperature on an 810 Material Test System (MTS) equipped with a 50 kN load cell. Stress was applied at a rate of 50 mm/min until the test specimens fractured. The ultimate strength, modulus, and strain at break was recorded for each sample tested. The ultimate strength was recorded as the maximum stress before fracture occurred. The modulus is the ratio of stress and strain observed before the specimen became permanently plastically deformed. The strain at break was recorded as the amount of strain at the point of specimen fracture.

ACKNOWLEDGEMENTS

Special thanks to assistance given by graduate student John Arnold and the many donors that generously gave to the University of New Orleans (UNO) Advanced Materials Research Institute (AMRI) High School Summer Research Program crowdfunding initiative. We also thank the Academy of Applied Science and AMRI for their support.

Received: December 8, 2019

Accepted: July 8, 2020

Published: July 17, 2020

REFERENCES

1. Gibson, Ian, et al. *Additive Manufacturing Technologies*. Springer New York, 2015. DOI.org (Crossref), doi:10.1007/978-1-4939-2113-3.
2. Mohamed, Omar A., et al. "Optimization of Fused Deposition Modeling Process Parameters: A Review of Current Research and Future Prospects." *Advances in Manufacturing*, vol. 3, no. 1, Mar. 2015, pp. 42–53. DOI.org (Crossref), doi:10.1007/s40436-014-0097-7.
3. Mohan, N., et al. "A Review on Composite Materials and Process Parameters Optimisation for the Fused Deposition Modelling Process." *Virtual and Physical Prototyping*, vol. 12, no. 1, Jan. 2017, pp. 47–59. DOI.org (Crossref), doi:10.1080/1

7452759.2016.1274490.

4 .Costa, Ana Elisa, et al. "A Study on Extruded Filament Bonding in Fused Filament Fabrication." *Rapid Prototyping Journal*, vol. 25, no. 3, Apr. 2019, pp. 555–65. DOI.org (Crossref), doi:10.1108/RPJ-03-2018-0062.

5. Khaliq, Muhammad Hussam, et al. "On the Use of High Viscosity Polymers in the Fused Filament Fabrication Process." *Rapid Prototyping Journal*, vol. 23, no. 4, June 2017, pp. 727–35. DOI.org (Crossref), doi:10.1108/RPJ-02-2016-0027.

6. Alafaghani, Ala'aldin, et al. "Design Consideration for Additive Manufacturing: Fused Deposition Modelling." *Open Journal of Applied Sciences*, vol. 07, no. 06, 2017, pp. 291–318. DOI.org (Crossref), doi:10.4236/ojapps.2017.76024.

7. Griffiths, C. A., et al. "Effect of Build Parameters on Processing Efficiency and Material Performance in Fused Deposition Modelling." *Procedia CIRP*, vol. 49, 2016, pp. 28–32. DOI.org (Crossref), doi:10.1016/j.procir.2015.07.024.

8. Hernandez, David. "Factors Affecting Dimensional Precision of Consumer 3D Printing." *International Journal of Aviation, Aeronautics, and Aerospace*, 2015. DOI.org (Crossref), doi:10.15394/ijaaa.2015.1085.

9. Torrado Perez, Angel R., et al. "Fracture Surface Analysis of 3D-Printed Tensile Specimens of Novel ABS-Based Materials." *Journal of Failure Analysis and Prevention*, vol. 14, no. 3, June 2014, pp. 343–53. DOI.org (Crossref), doi:10.1007/s11668-014-9803-9.

10. Carneiro, O. S., et al. "Fused Deposition Modeling with Polypropylene." *Materials & Design*, vol. 83, Oct. 2015, pp. 768–76. DOI.org (Crossref), doi:10.1016/j.matdes.2015.06.053.

11. Torres, Jonathan, et al. "An Approach for Mechanical Property Optimization of Fused Deposition Modeling with Polylactic Acid via Design of Experiments." *Rapid Prototyping Journal*, vol. 22, no. 2, Mar. 2016, pp. 387–404. DOI.org (Crossref), doi:10.1108/RPJ-07-2014-0083.

12. Wu, Wenzheng, et al. "Influence of Layer Thickness and Raster Angle on the Mechanical Properties of 3D-Printed PEEK and a Comparative Mechanical Study between PEEK and ABS." *Materials*, vol. 8, no. 9, Sept. 2015, pp. 5834–46. DOI.org (Crossref), doi:10.3390/ma8095271.

13. Górski, Filip, et al. "STRENGTH OF ABS PARTS PRODUCED BY FUSED DEPOSITION MODELLING TECHNOLOGY – A CRITICAL ORIENTATION PROBLEM." *Advances in Science and Technology Research Journal*, vol. 9, 2015, pp. 12–19. DOI.org (Crossref), doi:10.12913/22998624/2359.

Copyright: © 2020 Guan and Smith. All JEI articles are distributed under the attribution non-commercial, no derivative license (<http://creativecommons.org/licenses/by-nc-nd/3.0/>). This means that anyone is free to share, copy and distribute an unaltered article for non-commercial purposes provided the original author and source is credited.